

# Ultrafast intermolecular energy transfer in heavy water

L. Piatkowski<sup>#,\*</sup>, K. B. Eisenthal<sup>§</sup>, and H. J. Bakker<sup>#</sup>

<sup>#</sup>*FOM-Institute for Atomic and Molecular Physics,*

*Science Park 113, 1098 XG Amsterdam, The Netherlands*

<sup>§</sup>*Chemistry Department, Columbia University, New York, New York 10027, USA*

## Abstract

We report on a study of the vibrational energy relaxation and resonant vibrational (Förster) energy transfer of the OD vibrations of D<sub>2</sub>O and mixtures of D<sub>2</sub>O and H<sub>2</sub>O using femtosecond mid-infrared spectroscopy. We observe the lifetime of the OD vibrations of bulk D<sub>2</sub>O to be  $400 \pm 30$  fs. The rate of the Förster energy transfer is measured via the dynamics of the anisotropy of the OD vibrational excitation. For a solution of 0.5% D<sub>2</sub>O in H<sub>2</sub>O resonant energy transfer is negligible, and the anisotropy shows a single exponential decay with a time constant of  $2.6 \pm 0.1$  ps, representing the time scale of the molecular reorientation. With increasing concentration, the anisotropy decay becomes faster and non-exponential, showing the increased contribution of resonant energy transfer between the OD vibrations. We determine the Förster radius of the OD vibration of HDO in H<sub>2</sub>O to be  $r_0 = 2.3 \pm 0.2$  Å.

## I. INTRODUCTION

Resonant intermolecular energy transfer is an important process in nature that leads to delocalized excitations (excitons) and the equilibration of energy. This process is often denoted as Förster energy transfer after Theodor Förster. Förster energy transfer has been observed for electronic excitations<sup>1-3</sup> and vibrational excitations<sup>4-9</sup>. Well-known examples of systems showing resonant (Förster) vibrational energy transfer are the amide vibrations of polypeptides<sup>5</sup> and the OH stretch vibrations of liquid water<sup>6,7</sup>. The energy transfer is the result of a coupling between an excited oscillator and an oscillator in the ground state. In most cases, this coupling is formed by a dipole-dipole interactions which implies that the coupling is inversely proportional to the sixth power of the distance between the coupled oscillators.

For water the resonant coupling between the OH stretch vibrations has been studied by measuring the decay of the anisotropy of the excitation of the OH vibration for different isotopic mixtures of water and heavy water<sup>6</sup>. At a low concentration of water in heavy water (<1%) the OH groups are too far apart to show energy transfer within the vibrational lifetime of the OH stretch vibrations. In this dilute limit the anisotropy only decays as a result of the molecular reorientation of the water molecules. However, with increasing concentration of OH groups, the anisotropy decay is accelerated showing the presence of resonant energy transfer between OH groups that are differently oriented<sup>6-8</sup>. Up to high OH concentrations this resonant energy transfer could be well described with a dipole-dipole interaction mechanism, meaning that the rate scales inversely proportional to the sixth power of the distance between the OH groups. However, for pure liquid H<sub>2</sub>O the observed rate of resonant energy transfer was significantly faster than expected from the dipole-dipole interaction mechanism, indicating that higher-order multipole interactions also contribute to the energy transfer<sup>6</sup>.

Here we study the rate and mechanism of resonant vibrational energy transfer between OD vibrations in water. We measure the anisotropy dynamics of the OD vibration of pure D<sub>2</sub>O and of solutions of HDO dissolved in H<sub>2</sub>O for a large range of concentrations. We observe resonant energy transfer of the OD vibrations for all solutions for which the concentration of OD oscillators is larger than 1%.

## II. EXPERIMENT

We study the vibrational relaxation and resonant energy transfer of the OD stretch vibrations in water using femtosecond mid-IR pump-probe spectroscopy. In this technique, an IR pump pulse excites the OD vibration and the transient changes in absorption resulting from this excitation are monitored with a second IR pulse. The IR pulses are generated by frequency conversion processes that are pumped with the pulses derived from a high energy Ti:Sapphire amplifier system. This system is formed by a Coherent "Legend" regenerative amplifier and a custom-built cryo-multipass amplifier. The system provides 50 fs pulses, centered at a wavelength of 800 nm with a pulse energy of 6 mJ per pulse at a repetition rate of 1 kHz. We use about 1 mJ to pump an optical parametric amplifier (OPA). The produced signal pulses at about 1330 nm, 120 fs and an energy of 130  $\mu\text{J}$  are further amplified in a  $\beta$ -barium borate (BBO) crystal using the remaining 5 mJ pulses as a pump. The amplification process yields 700  $\mu\text{J}$  signal pulses and 400  $\mu\text{J}$  idler pulses centered at 2000 nm. The signal and idler are used in a difference frequency mixing process in silver gallium disulphide ( $\text{AgGaS}_2$ ) crystal resulting in 10  $\mu\text{J}$  pulses at 4000 nm, a pulse duration of about 70 fs, and a spectral bandwidth of  $\sim 450 \text{ cm}^{-1}$ .

The pulses are used in a one-color, polarization-resolved pump-probe experiment. In this experiment we measure the pump-induced frequency-resolved transient absorption spectra ( $\Delta\alpha$ ) of various samples as a function of time delay between pump and probe. The pump promotes population from the equilibrium ground state  $v = 0$  to the first excited state,  $v = 1$ . This excitation is observed as a bleach and stimulated emission at frequencies matching  $v = 0 \rightarrow 1$ , and an induced absorption at frequencies matching  $v = 1 \rightarrow 2$ . The probe is split off from the pump beam using a wedged  $\text{CaF}_2$  plate. The reflection from the front side is sent into a 4 fs resolution delay stage. The pump and probe are focussed to the same spot in the sample using a gold-coated parabolic mirror. The front reflection from a second wedged  $\text{CaF}_2$  plate is also focused in the sample by the same mirror, but not in overlap with the pump. This beam is used as a reference. After the sample, the probe and reference are dispersed with an Oriel monochromator and detected with the two lines of an Infrared Associates  $2 \times 32$  MCT (mercury-cadmium-telluride) detector array. The measurement of the reference thus allows for a frequency-resolved correction for shot-to-shot fluctuations of the probe-pulse energy.

Before entering the sample, the polarization of the probe is rotated at  $45^\circ$  with respect to the pump polarization using a half-wave plate. After the sample the polarization component parallel to

the pump or the component perpendicular to the pump can be selected using a polarizer mounted in a motorized rotation stage. The thus obtained transient absorption changes  $\Delta\alpha_{\parallel}(t)$  and  $\Delta\alpha_{\perp}(t)$  are used to construct the isotropic signal that is independent of the depolarization of the excitation:

$$\Delta\alpha_{iso}(t) = \frac{\Delta\alpha_{\parallel}(t) + 2 \cdot \Delta\alpha_{\perp}(t)}{3} \quad (1)$$

The isotropic signal  $\Delta\alpha_{iso}(t, \nu)$  gives information on the rate of vibrational energy relaxation.

The measured signals  $\Delta\alpha_{\parallel}(t)$  and  $\Delta\alpha_{\perp}(t)$  are also used to construct the so-called anisotropy parameter  $R(t)$  that only represent the dynamics of the depolarization of the excitation:

$$R(t) = \frac{\Delta\alpha_{\parallel}(t) - \Delta\alpha_{\perp}(t)}{3 \cdot \Delta\alpha_{iso}(t)} \quad (2)$$

The anisotropy parameter  $R(t)$  thus represents the normalized difference between parallel and perpendicular pump-probe polarizations and it can be shown that  $R(t)$  is proportional to the second-order autocorrelation function of the direction of the transition dipole moment.

We studied the vibrational relaxation and anisotropy dynamics for pure D<sub>2</sub>O and four mixtures of D<sub>2</sub>O and H<sub>2</sub>O. The samples were positioned between two 2 mm thick CaF<sub>2</sub> windows separated by teflon spacers with thicknesses ranging from 3.8  $\mu\text{m}$  to 100  $\mu\text{m}$ . To check a possible contribution of coherent artifacts to the signals at early delay times we also performed the experiment on pure D<sub>2</sub>O with 500 nm Si<sub>3</sub>N<sub>4</sub> membrane windows instead of 2 mm CaF<sub>2</sub> windows. From the comparison of the data sets we concluded that the coherent signal that originates from the CaF<sub>2</sub> windows is small and does not influence the fitted values for the lifetime and the anisotropy decay. During the experiment the samples were rotated to avoid accumulation of heat in the focus.

### III. RESULTS AND DISCUSSION

#### A. Vibrational relaxation

Figure 1 shows the linear spectra for pure D<sub>2</sub>O and mixtures of D<sub>2</sub>O and H<sub>2</sub>O. It is seen that an increase of the amount of H<sub>2</sub>O causes a narrowing of the D<sub>2</sub>O band. In addition, for the two lowest concentrations, we observe a background absorption. This background is caused by the low frequency part of the OH stretch vibrations of H<sub>2</sub>O and the high frequency part of the H<sub>2</sub>O combination band<sup>10</sup> centered around 2150  $\text{cm}^{-1}$ .

The OD vibration has a short lifetime and after a few picoseconds the vibrational energy becomes thermal which corresponds to a temperature increase of the sample in the focus. An increase

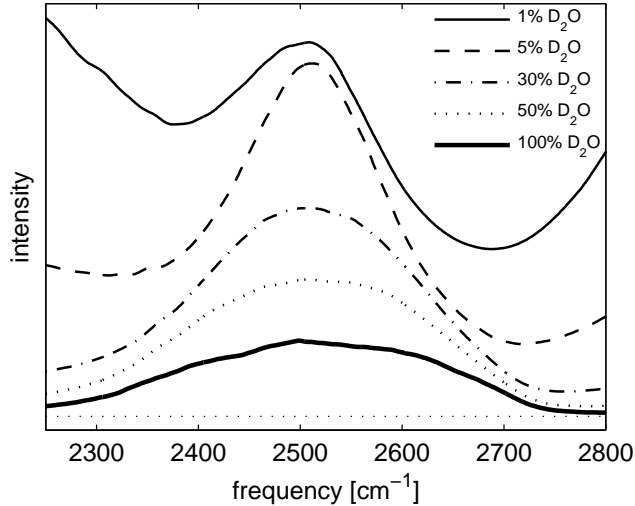


FIG. 1: Linear spectra of pure  $D_2O$  and mixtures of  $D_2O$  and  $H_2O$ . Spectra for higher  $D_2O$  concentrations have been scaled for clarity.

in temperature leads to a decrease of the cross-section and blueshift of the absorption spectrum of the OD stretch vibration. In the transient spectrum these effects correspond to a persistent bleaching in the red wing and center of the absorption band, and a small induced absorption in the blue wing of the absorption band. As this heating signal is isotropic, this signal should be subtracted from the measured transient spectra for a proper determination of the anisotropy dynamics of the vibrational excitation.

The subtraction of the heating signal is especially important for  $D_2O$  concentrations higher than 50%, since for these samples the heating signal is of comparable magnitude or bigger than the absorption changes originating from the population dynamics of the  $v = 1$  state. To determine the dynamics of the heating signal, we fit the isotropic signals to a two-step relaxation model. In this model the vibrational energy of the excited  $v = 1$  state is first transferred to a non-thermal intermediate state. In the second step the intermediate state relaxes leading to a full thermalization of the energy. The rate of the first step is characterized by a vibrational lifetime  $T_1$ , the second step by an equilibration time constant  $T_*$ . As has been shown before<sup>11</sup> the fit of the data to this model thus provides us with the contribution of the heating signal to the measured absorption changes at all delay times. Such obtained isotropic heat signal is then subtracted from the overall signal. The transient absorption spectrum for pure  $D_2O$  corrected for the heating effect is shown in figure 2 for two delay times. From the fit we obtain a vibrational lifetime  $T_1$  of  $400 \pm 30$  fs for pure  $D_2O$  and

a heat ingrowth time  $T_*$  of  $630 \pm 50$  fs. The lifetime of  $400 \pm 30$  fs agrees well with the value of  $350 \pm 50$  fs reported by Volkov et al.<sup>12</sup>.

We used the same fitting procedure for all  $D_2O/H_2O$  mixtures. For the two lowest concentrations (1% and 5% of  $D_2O$  in  $H_2O$ ) the fit resulted in a vibrational lifetime for the isolated OD vibration  $T_1$  of  $1.7 \pm 0.1$  ps and a heat ingrowth time  $T_*$  of  $850 \pm 50$  fs.

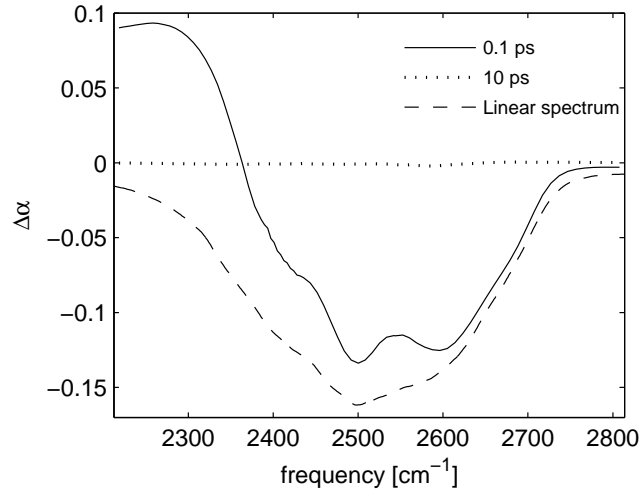


FIG. 2: Transient spectra of pure  $D_2O$  recorded at 0.1 ps and 10 ps. Linear spectrum of pure  $D_2O$  is shown with the dashed line.

The intermediate state represents a state of the system in which the energy is no longer residing in the excited  $v = 1$  state, in which the energy has also not yet become thermally distributed. The intermediate state likely represents specific combined excitations of low-frequency modes. The occupation of these modes can induce an anharmonic frequency shift of the absorption spectrum of studied vibration. In this case the transient spectrum associated with the intermediate state will consist of a bleaching and an induced absorption signal of which the magnitude are determined by the amount of the anharmonic frequency shift. From the spectral decomposition we find however that the intermediate state in the relaxation of the OD vibration does not have such an associated spectrum. In fact, the intermediate state has the same absorption spectrum as the ground state of the OD vibration. This means that the transient occupation of the intermediate state only functions to describe the delay in rise of the spectral responses that are characteristic for a heating of the sample. The spectral changes associated with the heating of the sample are largely due to the weakening of the hydrogen bonds between the water molecules. Hence, the time constant  $T_*$  likely represents the time scale at which the hydrogen bonds adapt to an ultrafast local dissipation of energy. This adaptation is relatively slow as the frequencies of the hydrogen-bond vibrations are low. This type of behavior can be expected to occur in all systems in which the intermolecular dynamics is not much faster than the relaxation of the excited state of a high-energy degree of freedom and in which the intermolecular dynamics have a strong effect on the absorption spectrum of the high-energy degree of freedom. Water is a clear example showing this type of behavior.

## **B. Förster energy transfer**

Figure 3 shows the anisotropy decays as a function of delay for pure  $D_2O$  and for four mixtures of  $D_2O/H_2O$ . The decay of the anisotropy reflects both the effects of molecular reorientation and resonant energy transfer between differently oriented OD groups. The two effects can be distinguished by varying the concentration of OD oscillators. For the lowest concentration (1% of  $D_2O$  in  $H_2O$ ) the contribution of the energy transfer to the decay of the anisotropy is very small and the anisotropy decays mainly because of the molecular reorientation of the HDO molecules. The observed decay can be fitted well with a single exponential with a time constant  $\tau$  of  $2.6 \pm 0.1$  ps. This reorientation time constant agrees well with previous reports<sup>11,13,14</sup>. With increasing concentration of  $D_2O$ , we observe the depolarization of the OD oscillators to become faster, showing the contribution of Förster energy transfer to the anisotropy decay.

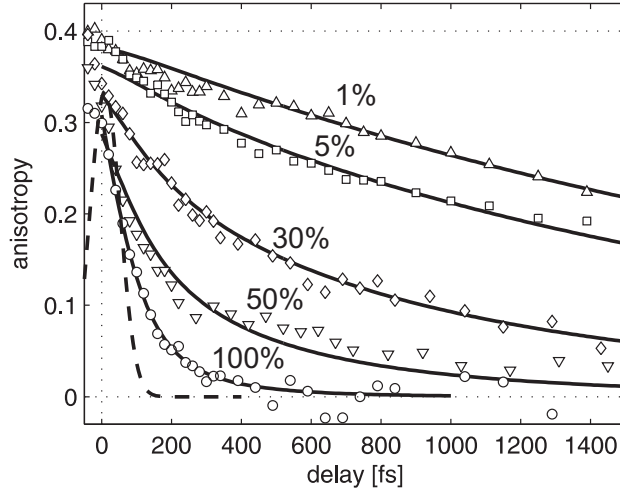


FIG. 3: Orientational anisotropy decay curves for different concentrations of  $D_2O$  in  $H_2O$ . The result of the fits to equation 8 are represented by the solid curves. The dashed line represents a gaussian profile fitted to the cross-correlated signal of pump and probe pulses.

In the presence of intermolecular energy transfer, the anisotropy dynamics can be described with the formula<sup>15,16</sup> developed by Förster in the 1940's:

$$R(t) = \exp\left(-\frac{t}{\tau_{or}} - \frac{4\pi^{3/2}}{3} [OD] \sqrt{\frac{r_0^6 t}{T_1}}\right), \quad (3)$$

where  $\tau_{or}$  is the reorientation time and  $[OD]$  is the concentration of OD moieties in the system. An essential parameter in equation (3) is  $r_0$ , the so-called Förster radius. This parameter denotes the distance at which the energy transfer efficiency is 50%. In other words, at this distance, 50% of molecules will transfer their vibrational energy via dipole-dipole interactions within the vibrational lifetime.

Equation (3) was derived assuming a statistical distribution of distances between the exchanging molecules. As a result, the transfer rate is strongly time dependent (as expressed in the square-root dependence on time in the exponent of equation (3)). At short times, the rate is high due to transfers between OD vibrations that are at a close distance. With increasing time the transfer rate decreases, as the transfer becomes increasingly dominated by energy transfer between OD vibrations that are at a large mutual distance. The derivation of equation (3) can be found in the original work by Förster<sup>15</sup>. In the derivation of equation (3) it is also assumed that the exchanging OD vibrations have a random relative orientation. This assumption is not completely correct, because

the structure of the hydrogen-bond network of water will lead to an angular correlation of OD groups that are at a small mutual distance.

Equation 3 provides a good description of the experimentally determined  $R(t)$  in case the reorientation and the characteristic time scale of the Förster energy transfer are short compared to the instrument response function, i. e. the cross-correlation of the pump and probe pulses. For dynamics that are comparable with the time duration of the cross-correlate, the measured response includes the instrument response function. Unfortunately, the effect of the limited time resolution of the experiment cannot be accounted for by comparing the experimentally determined  $R(t)$  with a convolution of equation 3 and the cross-correlate of pump and probe, as the experimental  $R(t)$  anisotropy is not measured directly but constructed from the measured  $\Delta\alpha_{\parallel}(t)$  and  $\Delta\alpha_{\perp}(t)$ . Hence the instrument response has to be accounted for in the separately measured  $\Delta\alpha_{\parallel}(t)$  and  $\Delta\alpha_{\perp}(t)$ . The isotropic absorption change is given by:

$$\Delta\alpha_{\text{iso}}(t) = \int P(\tau)G(t - \tau)d\tau, \quad (4)$$

with  $G(t - \tau)$  being the instrument response function and  $P(\tau)$  the population relaxation function. The function  $P(\tau)$  can be a single exponential, i.e.  $e^{-\tau/T_1}$ , but it can also be more complicated if the relaxation process involves more than two states. We can construct model parallel and perpendicular responses from:

$$\Delta\alpha_{\parallel}(t) = \Delta\alpha_{\text{iso}}(t) + \frac{2}{3} \int R(\tau)P(\tau)G(t - \tau)d\tau, \quad (5)$$

and

$$\Delta\alpha_{\perp}(t) = \Delta\alpha_{\text{iso}}(t) - \frac{1}{3} \int R(\tau)P(\tau)G(t - \tau)d\tau \quad (6)$$

At this point both signals are modulated by the function  $R(\tau)$  which reflects the anisotropy decay. This function corresponds to equation (3). The difference between the two signals is then defined as:

$$\Delta\alpha_{\parallel}(t) - \Delta\alpha_{\perp}(t) = \int R(\tau)P(\tau)G(t - \tau)d\tau \quad (7)$$

The expression for the model anisotropy  $R_{\text{mod}}(t)$  is thus

$$R_{\text{mod}}(t) = \frac{\int R(\tau)P(\tau)G(t - \tau)d\tau}{\Delta\alpha_{\text{iso}}(t)} \quad (8)$$

Clearly, the expression for  $R_{\text{mod}}(t)$  is not the same as  $\int R(\tau)G(t - \tau)d\tau$ . The difference is negligible for a slowly decaying anisotropy, however, it becomes significant when  $R(\tau)$  shows dynamics on the same scale as the cross-correlation. To determine the Förster radius  $r_0$  expression 8

is fitted to the experimentally determined  $R(t)$ . All curves can be described well by equation 8. The function  $G(t - \tau)$  represents a gaussian fit to the experimental cross-correlation and  $P(\tau)$  is a monoexponential population decay with a  $T_1$  value that follows from the isotropic data. Fitting the data to equation 8 using a least-squares fitting method yields a value for the Förster radius  $r_0$  of  $2.3 \pm 0.2 \text{ \AA}$ , which is very similar to the value found previously for the OH stretch vibration in water<sup>6</sup>.

Figure 3 shows that the anisotropy decay observed for a solution of 5%  $D_2O$  in  $H_2O$  significantly differs from that observed for a solution of 1%  $D_2O$  in  $H_2O$ . For the solution containing 5%  $D_2O$  the anisotropy is observed to decay to a much lower level in the first 400 fs after the excitation. This finding shows that Förster energy transfer already plays a role at this concentration at which the average distance between the OD oscillators is approximately  $6 \text{ \AA}$ .

To study the contribution of Förster energy transfer to the anisotropy dynamics for low concentrations at early delays, we have performed additional experiments on four samples of 0.5%, 1%, 3% and 5% of  $D_2O$  in  $H_2O$ . The results are shown in figure 4. We have fitted the data with a single exponential function between 0.3 ps and 8 ps and found that at all concentrations the decay can be fitted well with a time constant of  $2.6 \pm 0.1 \text{ ps}$ . However, there is a significant effect in the extrapolated starting value of the single exponential fit at delay zero. Decreasing the amount of  $D_2O$  resulted in an increase of the starting value for the anisotropy from 0.35 for a 5% mixture up to 0.39 for a 0.5% mixture.

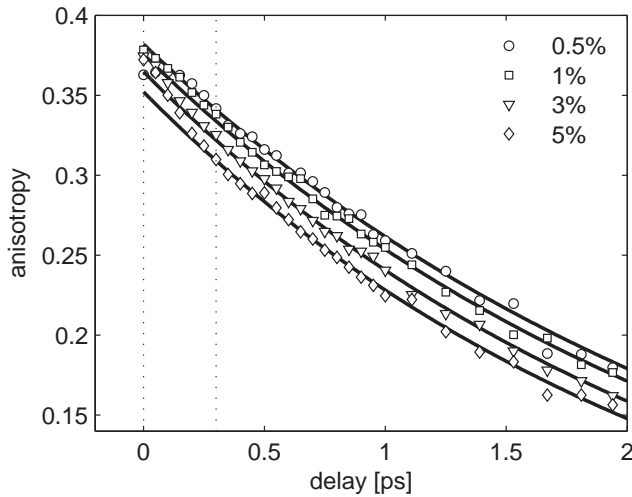


FIG. 4: Anisotropy decay curves for low concentrations of  $D_2O$  in  $H_2O$ . The result of the fits to monoexponential function are represented by the solid curves.

Using equation 3 we can determine the contribution of Förster energy transfer to the decay of the anisotropy. We rewrite formula 3 in a form  $R(t) = \exp(-R - F)$ , where  $R$  and  $F$  represent the orientational relaxation and the energy transfer contributions. In figure 5 we plot the function  $1 - \exp(-F)$  as a function of the concentration of  $D_2O$  at a delay of 0.4 ps. This function represents the decay of the anisotropy in case there would only be Förster energy transfer. For delays  $< 0.5$  ps this function provides a good approximation of the contribution of Förster energy transfer to the overall anisotropy decay, because in this time interval the change of the anisotropy due to orientational relaxation is small. The inset in figure 5 shows the amount of energy transfer at very low  $D_2O$  concentrations. The open circles correspond to the concentrations used in the experiment. It follows that energy transfer contributes to the anisotropy decay even for a solution of 0.5%  $D_2O$  in  $H_2O$ .

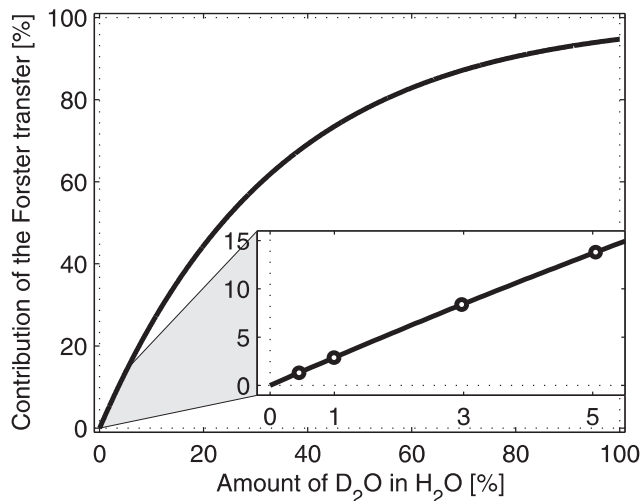


FIG. 5: Anisotropy decay due to Förster energy transfer only at 0.4 ps. The contribution is calculated using equation 3 with parameters derived from the experimental results.

From the results of figure 4 it follows that for solutions containing 3% and 5%  $D_2O$  Förster energy transfer leads to a decay of the anisotropy up to  $\sim 20\%$  in the first 400 fs after the excitation. Fast initial anisotropy decays have been observed before for mixtures of  $D_2O$  and  $H_2O$ <sup>11,13,14</sup>, but these initial decays were assigned to librational motions that keep the  $O-H \cdots O$  hydrogen bond intact. However, the present comparison of the results obtained for 5%  $D_2O$  in  $H_2O$  and 0.5%  $D_2O$  in  $H_2O$  shows that a significant part of this initial decay is in fact due to Förster energy transfer. Librational motions are certainly expected to be present in liquid water and to contribute to a fast initial decay of the anisotropy<sup>17</sup>, but their amplitude is smaller than has been reported<sup>11,13,14</sup>.

For pure D<sub>2</sub>O, a significant part of the energy transfer will take place between the two OD vibrations within the D<sub>2</sub>O molecule. In a recent experimental and theoretical study of the intra- and intermolecular couplings of H<sub>2</sub>O it was found that the spectral dynamics of the OH stretch vibrations of H<sub>2</sub>O mainly result from this intramolecular coupling<sup>18</sup>. However, with respect to the anisotropy, the intramolecular coupling can only account for a partial decay, as intramolecular energy transfer only leads to the equilibration of the energy in the plane of the molecule. Hence, the observed complete rapid decay of the anisotropy shows that for D<sub>2</sub>O fast intermolecular energy transfer processes must be present.

The process of Förster energy transfer in water has been studied before for the OH stretch vibrations of solutions of HDO in D<sub>2</sub>O<sup>6</sup> and for pure H<sub>2</sub>O<sup>6-8</sup>. From the measurements on HDO in D<sub>2</sub>O, the Förster radius was determined to be 2.1 Å, which is very comparable to the Förster radius of 2.3±0.2 Å we find here for the OD vibration in water. To compare the Förster energy transfer rates of the OD and the OH vibrations in water we use:

$$k_F(r) = \frac{1}{T_1} \left( \frac{r_0}{r} \right)^6 \quad (9)$$

The values of  $T_1$  of the OH vibration of HDO in D<sub>2</sub>O is 740 fs<sup>19</sup> and of the OD vibration of HDO in H<sub>2</sub>O is 1.7 ps. Assuming that the values of  $r_0$  are the same for OD and OH, we thus find that  $k_{F,OH}(r) \approx 2.3k_{F,OD}(r)$ .

The ratio of the Förster energy transfer rates of the OD and OH vibrations in water can be compared to the ratio that follows from the linear absorption spectra of these vibrations assuming that the energy transfer results from a dipole-dipole interaction mechanism. In this case the Förster energy transfer rate between the same type of oscillators is given by<sup>19,20</sup>:

$$k_F(r) \sim \frac{\sigma^2}{r^6} \int g^2(\nu) d\nu, \quad (10)$$

where  $\sigma$  denotes the cross-section and  $g(\nu)$  the absorption line profile. The cross-section of the OD vibration of HDO in H<sub>2</sub>O is approximately 1.9 times smaller than that of the OH vibration of HDO in D<sub>2</sub>O. Another difference between the linear absorption spectra is that the frequency axis of the OD vibration is contracted by a factor of  $\sim \sqrt{2}$ . If we assume the line shapes of the OH and the OD vibrations to be Gaussian, it follows from equation 10 that  $k_{F,OH}(r) \approx (1.9^2/\sqrt{2})k_{F,OD}(r) \approx 2.55k_{F,OD}(r)$ . This ratio compares very well with the experimentally observed ratio of  $\sim 2.3$ , which corroborates that the energy transfer among the OD vibrations of HDO in H<sub>2</sub>O indeed

relies on a dipole-dipole interaction mechanism.

For pure H<sub>2</sub>O the resonant energy transfer among the OH vibrations was observed to be significantly faster than expected from an extrapolation of the dipole-dipole interaction of the OH vibrations of solutions of HDO in D<sub>2</sub>O<sup>6</sup>. Possible explanations for this deviation are a break-down of the dipole-dipole description, i. e. the presence of additional multi-pole electric field interactions and the contribution of (intramolecular) anharmonic couplings to the energy transfer. Interestingly, this behavior is not observed for pure D<sub>2</sub>O. The observed anisotropy decay of pure D<sub>2</sub>O can be quite well accounted for using the same dipole-dipole coupling that accounts for the anisotropy decay of the solutions of HDO in H<sub>2</sub>O (figure 3). This finding indicates that intramolecular anharmonic couplings of the OD vibrations do not contribute to the energy transfer within the D<sub>2</sub>O molecule. In addition, this finding suggests that for D<sub>2</sub>O the dipole-dipole approximation of the intramolecular electrostatic interaction remains valid.

#### IV. CONCLUSIONS

We study the vibrational energy relaxation and resonant Förster energy transfer dynamics of the OD stretch vibrations in pure D<sub>2</sub>O and solutions of HDO in H<sub>2</sub>O with polarization-resolved femtosecond mid-infrared pump-probe spectroscopy employing 70 fs pulses with a central wavelength of 4  $\mu$ m. The vibrational relaxation of the OD vibration of pure D<sub>2</sub>O is observed to occur with a time constant of  $400 \pm 30$  fs.

We monitor the occurrence of Förster resonant energy transfer of the OD vibrations by measuring the dynamics of the anisotropy of the vibrational excitation of the OD vibration for different concentrations of HDO in D<sub>2</sub>O. With increasing HDO concentration the anisotropy decay accelerates and becomes increasingly non-exponential. These observations can be modeled well with a resonant energy transfer model in which the OD vibrations interact via a dipole-dipole coupling mechanism. From a fit to the data obtained at different concentrations we determine the Förster radius  $r_0$  to be  $2.3 \pm 0.2$  Å. The rate constant of the Förster energy transfer is observed to be  $\sim 2.3$  times smaller than for the OH vibrations of HDO dissolved in D<sub>2</sub>O. This ratio is fully consistent with a dipole-dipole interaction mechanism and can be well explained from the difference in cross-section and spectral distribution of the OD and the OH stretch vibrations.

We observe that the Förster energy transfer already significantly contributes to the decay of the anisotropy of the OD vibration for D<sub>2</sub>O concentrations  $\leq 5\%$ . At these concentrations, the

resonant energy transfer is observed to induce a fast partial decay of the anisotropy in the first 400 fs after the vibrational excitation. For a D<sub>2</sub>O concentrations of 5% this fast initial decay amounts to ~20% of the anisotropy decay. This result implies that previous observations of a fast initial anisotropy decay for the same system are only partly the result of librational motions.

For pure D<sub>2</sub>O the Förster energy transfer can be well described with the same dipole-dipole interaction mechanism that accounts for the energy transfer in solutions of HDO in H<sub>2</sub>O. This result indicates that for D<sub>2</sub>O, in contrast to H<sub>2</sub>O<sup>6</sup>, the description of the intramolecular electrostatic interaction of the stretch vibrations does not require the inclusion of higher-order multipole interactions.

### **Acknowledgments**

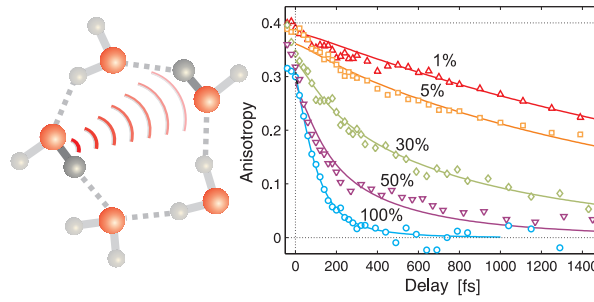
This work has been financially supported by the European Union - Marie Curie program (MEST-CT-2005-021000). The work is also part of the research program of the Foundation for Fundamental Research on Matter (FOM) which is financially supported by the Dutch organization for Scientific Research (NWO). KBE would like to thank NSF, Office of Basic Energy Sciences DOE, DTRA(W911NF-07-1-0116). The authors would like to thank H. Schoenmaker and A. de Snaijer for technical support and R.L.A. Timmer for stimulating discussions.

---

\* Electronic address: l.piatkowski@amolf.nl

- <sup>1</sup> R. Bennet, R. P. Schwenker and R. Kellog, *J. Chem. Phys.*, 1964, **41**, 3037.
- <sup>2</sup> D. Rehm and K. E. Eissenthal, *Chem. Phys. Lett.*, 1971, **9**, 387.
- <sup>3</sup> J. M. Drake, J. Klafter and L. P., *Science*, 1991, **251**, 1574.
- <sup>4</sup> M. P. J. Brugmans, H. J. Bakker and L. A., *J. Chem. Phys.*, 1996, **104**, 64.
- <sup>5</sup> C. Fang, A. Senes, L. Cristian, W. F. DeGrado and R. M. Hochstrasser, *PNAS*, 2006, **103**, 16740.
- <sup>6</sup> S. Woutersen and H. J. Bakker, *Nature*, 1999, **402**, 507–509.
- <sup>7</sup> M. L. Cowan, B. D. Bruner, N. Huse, J. R. Dwyer, B. Chugh, E. T. J. Nibbering, T. Elsaesser and R. J. D. Miller, *Nature*, 2005, **434**, 199.
- <sup>8</sup> D. Kraemer, C. M. L., A. Paarmann, N. Huse, E. T. J. Nibbering, T. Elsaesser and R. J. D. Miller, *PNAS*, 2008, **105**, 437–442.
- <sup>9</sup> J. A. Poulsen, G. Nyman and S. Nordholm, *J. Phys. Chem.*, 2003, **107**, 8420.
- <sup>10</sup> A. Millo, Y. Raichlin and A. Katzir, *Appl. Spec.*, 2005, **59**, 460–466.
- <sup>11</sup> Y. L. A. Rezus and H. J. Bakker, *J. Chem. Phys.*, 2005, **123**, 114502.
- <sup>12</sup> V. V. Volkov, D. Palmer and R. Righini, *J. Phys. Chem. B*, 2007, **111**, 1377.
- <sup>13</sup> H. J. Bakker, Y. L. A. Rezus and R. L. A. Timmer, *J. Phys. Chem. A*, 2008, **112**, 11523–11534.
- <sup>14</sup> D. E. Moilanen, E. E. Fenn, Y. Lin, J. L. Skinner, B. Bagchi and M. D. Fayer, *PNAS*, 2008, **105**, 5295.
- <sup>15</sup> T. Förster, *Z. Naturforschg.*, 1940, **4**, 821–827.
- <sup>16</sup> S. E. Braslavsky, E. Fron, H. B. Rodriguez, E. San Roman, G. Scholes, G. D. and Schweitzer, B. Valeur and J. Wirz, 2008, **7**, 1444.
- <sup>17</sup> A. D. Laage and J. T. Hynes, *Chem. Phys. Lett.*, 2006, **433**, 80–85.
- <sup>18</sup> A. Paarmann, T. Hayashi, S. Mukamel and R. J. D. Miller, *J. Chem. Phys.*, 2008, **128**, 191103.
- <sup>19</sup> S. Woutersen, U. Emmerichs and H. J. Bakker, *J. Chem. Phys.*, 1997, **107**, 1483–1490.
- <sup>20</sup> M. Morin, P. Jakob, N. J. Levinos, Y. J. Chabal and A. L. Harris, *J. Chem. Phys.*, 1992, **96**, 6203–6212.

## Graphical abstract



We have studied resonant (Förster) energy transfer between the OD oscillators in mixtures of D<sub>2</sub>O/H<sub>2</sub>O and pure D<sub>2</sub>O by means of polarization and time resolved mid-IR spectroscopy.